A role for the dynamin-like protein Vps1 during endocytosis in yeast

Iwona I. Smaczynska-de Rooij[1], Ellen G. Allwood[1], Soheil Aghamohammadzadeh[1], Ewald H. Hettema[1], Martin W. Goldberg[2] and Kathryn R. Ayscough[1,*]

[1]Department of Molecular Biology and Biotechnology, Firth Court, University of Sheffield, Sheffield S10 2TN, UK
[2]School of Biological and Biomedical Sciences, Durham University, Durham DH1 3LE, UK
*Author for correspondence (k.ayscough@sheffield.ac.uk)

Accepted 30 June 2010
Journal of Cell Science 123, 3496-3506

doi:10.1242/jcs.070508

Summary

Dynamins are a conserved family of proteins involved in membrane fusion and fission. Although mammalian dynamins are known to be involved in several membrane-trafficking events, the role of dynamin-1 in endocytosis is the best-characterised role of this protein family. Despite many similarities between endocytosis in yeast and mammalian cells, a comparable role for dynamins in yeast has not previously been demonstrated. The reported lack of involvement of dynamins in yeast endocytosis has raised questions over the general applicability of the current yeast model of endocytosis, and has also precluded studies using well-developed methods in yeast, to further our understanding of the mechanism of dynamin function during endocytosis. Here, we investigate the yeast dynamin-like protein Vps1 and demonstrate a transient burst of localisation to sites of endocytosis. Using live-cell imaging of endocytic reporters in strains lacking *vps1*, and also electron microscopy and biochemical approaches, we demonstrate a role for Vps1 in facilitating endocytic invagination. Vps1 mutants were generated, and analysis in several assays reveals a role for the C-terminal self-assembly domain in endocytosis but not in other membrane fission events with which Vps1 has previously been associated.

Key words: Dynamin, Amphiphysin, Endocytosis, Rvs167, *Saccharomyces cerevisiae*

Introduction

Endocytosis is a highly regulated and essential process that occurs in the majority of eukaryotic cells. It is required for recycling of plasma membrane lipids and trafficking proteins, and for uptake or downregulation of cell-surface receptors. During endocytosis, the plasma membrane invaginates into the cell, resulting in the production of a vesicle that is then able to fuse with endosomes and enter the endolysosomal membrane system. This process is known to involve more than 50 proteins, which assemble transiently at sites on the plasma membrane (for a review, see Robertson et al., 2009).

Work in the model organism *Saccharomyces cerevisiae* has led to significant advances in our understanding of the distinct stages that take place during endocytosis in vivo. It is now widely believed that the broad stages of coat assembly (early), invagination (mid) and scission, followed by inward movement (late) are largely conserved across evolution, and that in many cases direct homologues of proteins are responsible for carrying out the same steps in the process. One notable difference between yeast and mammalian cells is that dynamins are considered to be central to the endocytic process in mammalian cells, whereas this family of proteins has been considered to be largely peripheral to endocytic function in yeast (Gammie et al., 1995; Yu and Cai, 2004).

Dynamin was originally isolated 20 years ago as a microtubule-binding protein (Shpetner and Vallee, 1989). A role in endocytosis was indicated from studies in *Drosophila*, when mutations in the *shibire* gene were seen to cause paralysis at an elevated temperature by reversibly blocking endocytosis at the nerve terminal (Koenig and Ikeda, 1989). *Shibire* was subsequently identified as *Drosophila* dynamin (Chen et al., 1991; Van Der Bliek and Meyerowitz, 1991). Although mammalian dynamins have been shown to be crucial for endocytic function, their exact mechanism of function has remained the subject of debate (Song and Schmid, 2003). Furthermore, the presence of several mammalian dynamin genes (*DNM1*, *DNM2* and *DNM3*) adds additional complexity. Although dynamin-1 is thought to have a role solely in endocytosis, dynamin-2 is considered to have a broader role possibly involving the *trans*-Golgi network, endosomes and podosomes, as well as endocytosis (Cao et al., 2003; Cao et al., 2005; Ferguson et al., 2009; Ochoa et al., 2000), whereas the role for dynamin-3 is still largely unknown, although this protein has a more restricted tissue expression (Kruchten and McNiven, 2006). For several years, dynamin-1 was proposed to act largely in a mechanical way to encircle the neck of invaginated endocytic vesicles facilitating scission of vesicles during endocytosis (Hinshaw and Schmid, 1995). Subsequently, a regulatory role was described, in which dynamin functions earlier through its GTPase domain as a molecular switch to regulate recruitment or activity of proteins within the endocytic complex (Sever et al., 1999). Other studies have indicated that dynamin might function in both a regulatory and mechanical manner (Narayanan et al., 2005). A recent study of dynamin-1- and dynamin-2-knockout cells suggests a predominant role for dynamin in scission rather than earlier events, and has also revealed the importance of amphiphysins and actin in mammalian endocytosis (Ferguson et al., 2009).

Yeast contains three dynamin homologues (Vps1, Dnm1 and Mgm1), all of which contain the crucial N-terminal GTPase domain, a middle domain and a GTPase effector domain (GED) at the C-terminus, which has also been shown to function in oligomerisation. Similar to other dynamin-like proteins, Vps1 does not contain the PH domain, nor the C-terminal proline-rich domain, which is found in conventional dynamins (Shin et al., 1999; Vater

et al., 1992). Vps1 is involved in several membrane fusion and fission events within the Golgi, vacuole, endosome and peroxisomal systems (Hoepfner et al., 2001; Kuravi et al., 2006; Nothwehr et al., 1995; Peters et al., 2004; Vater et al., 1992), whereas Dnm1 and Mgm1 are thought to be involved in mitochondrial fusion and fission (Cerveny et al., 2007). However, a role for Dnm1 in endosomal trafficking has also been reported (Gammie et al., 1995). A role for Vps1 in early stages of endocytosis has been controversial and it is rarely listed as a protein involved in the yeast endocytic process. However, there is evidence that deletion of *VPS1* affects the morphology of cortical actin patches and that it interacts with an endocytic adaptor protein Sla1 (Yu and Cai, 2004). It is possible that the role for dynamins in yeast endocytosis has been underestimated because of their involvement in other cell processes, and also the ability of cells to undergo endocytosis in their absence.

In yeast, it is the amphiphysin proteins (Rvs167 and Rvs161) that have been considered responsible for vesicle scission. Similarly to dynamins, amphiphysins have the ability to tubulate and fragment membranes in vitro (Dawson et al., 2006). In addition to this mechanical role, the SH3 domain at the C-terminus of some amphiphysins (including Rvs167) is likely to be important in recruiting and possibly activating other endocytic proteins. Deletion of *RVS167* causes a reduction (~30%) in the number of successful vesicle scission events (Kaksonen et al., 2005), indicating that the amphiphysins are important, but might not be the only proteins involved in this event.

Results

Vps1 colocalises with endocytic proteins

Vps1 has a clearly demonstrated role in endosomal trafficking and in peroxisomal fission (Hoepfner et al., 2001; Nothwehr et al., 1995; Vater et al., 1992; Peters et al., 2004; Rothlisberger et al., 2009). In this study, we aimed to determine whether this fusion–fission role also functions during endocytosis. A minimum requirement for a protein to a have a direct role in endocytosis is for it to show at least partial localisation to endocytic sites. In previous studies, Vps1 has been shown to localise to internal organelles, and this staining is predominant in cells expressing GFP-tagged Vps1 (Peters et al., 2004). However, partial colocalisation with an endocytic adaptor protein Sla1 has also been reported (Yu and Cai, 2004). Expression of Vps1-GFP from both high and low copy number plasmids leads to high levels of fluorescence on the internal membranes and in these cells, spots at the cell periphery are difficult to discern (our unpublished observations). In this study, we have used a strain expressing Vps1-GFP under its own promoter (Peters et al., 2004). Vps1-GFP was expressed, both as the sole source of Vps1 in a haploid cell, and also coexpressed with endogenous untagged Vps1 in a heterozygous diploid cell. In both strains, the behaviour of coexpressed RFP markers are apparently normal, and do not show the aberrant behaviours observed for the *vps1*-deletion strain (see below). To investigate colocalisation with endocytic markers, cells were generated that coexpress Vps1-GFP and either Sla1-mRFP (a marker that is present throughout endocytic invagination) or Abp1mRFP (a marker of actin at the site). These strains were analysed using both wide-field epifluorescence microscopy and TIRF microscopy. As shown in Fig. 1A (upper panels), Vps1GFP was found in several internal organelles, which are likely to be endosomes. It also colocalised with Abp1mRFP, demonstrating that Vps1 is present at endocytic sites. By TIRF microscopy,

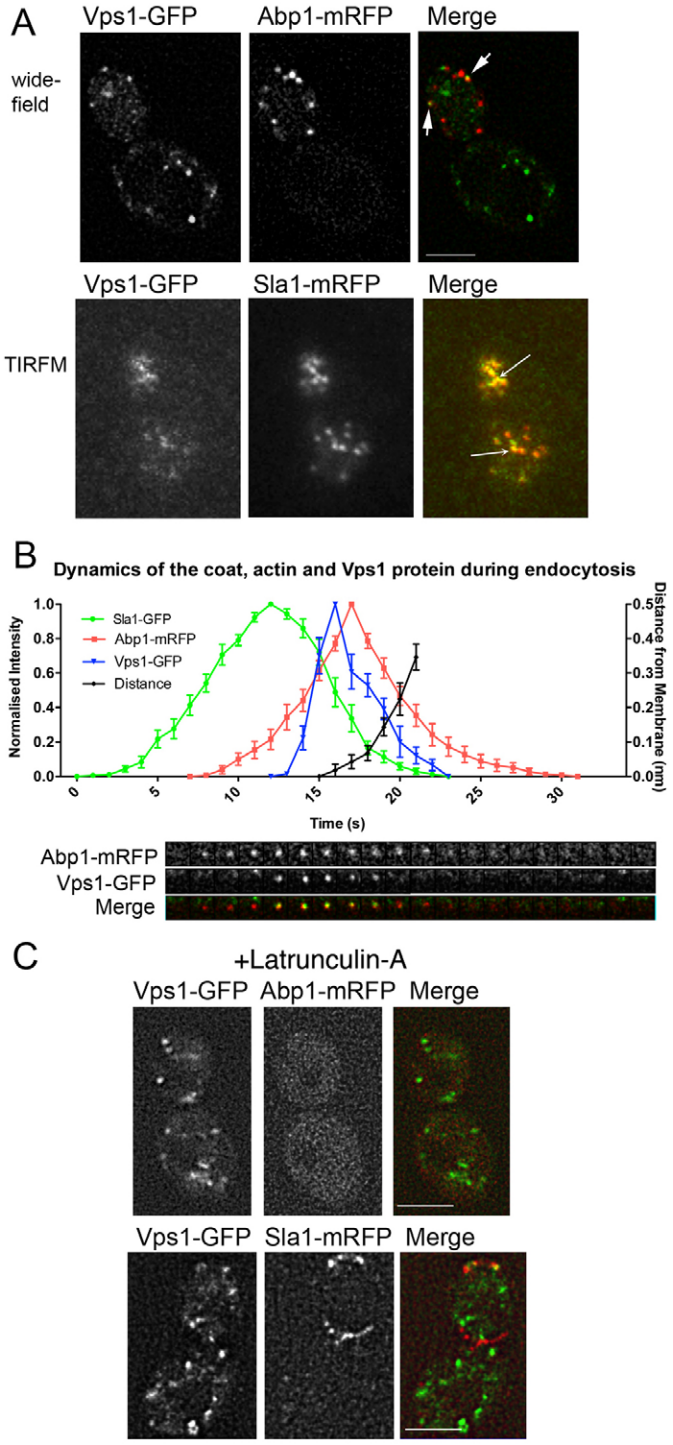

Fig. 1. Vps1 colocalises with endocytic proteins. (**A**) Vps1-GFP and either Abp1-mRFP (upper) or Sla1-mRFP (lower) were coexpressed and cells imaged. Arrows depict merged spots. Scale bar: 2 µm. (**B**) Vps1-GFP was coexpressed with Abp1-mRFP and intensity curves generated for eight separate endocytic spots. Weighted averages of spot intensity was calculated and plotted (means ± s.d.). The accompanying images for one of these spots are shown below the graph. Sla1-GFP was also expressed with Abp1-mRFP and intensity curves generated to allow relative comparisons. The distance of the tip of the Abp1 spots from the membrane were plotted. (**C**) 200 µM Lat-A was added to cells coexpressing Vps1-GFP with Abp1-mRFP (upper) or Sla1-mRFP (lower). Scale bars: 2 µm.

colocalisation with the coat protein Sla1-mRFP was also clear. However, colocalisation with both markers was only partial, suggesting that either only a subset of sites recruit Vps1 or that Vps1 is present only transiently at endocytic sites. To address this, the timing of Vps1 localisation was measured relative to the actin marker Abp1. Intensity profiles of multiple spots were generated (Fig. 1B). This approach revealed that Vps1 arrived about 5–6 seconds after Abp1, at a time corresponding to onset of invagination (Fig. 1B) (Liu et al., 2009). Vps1 then remained at the membrane and disassembled from the site before Abp1. Vps1 lifetime at the membrane was 8.70±4.07 seconds (mean ± s.d.; *n*=75 patches). This lifetime was the same whether Vps1-GFP was expressed as the sole form of Vps1, or coexpressed with untagged endogenous Vps1. The Vps1 lifetime corresponds to about half the lifetime of Abp1 at patches (Abp1 lifetime ~18 seconds) and about one third of the lifetime of Sla1 (25–30 seconds) and can explain why only partial colocalisation with these endocytic markers was observed.

A characteristic feature of many endocytic proteins is that their lifetime at the plasma membrane is increased in the presence of the actin-monomer-sequestering drug latrunculin A (Lat-A) (Ayscough et al., 1997; Morton et al., 2000; Toshima et al., 2009). Although actin-binding proteins are unable to assemble at the site, actin-independent components localise, and remain at sites for longer. Lat-A was added to cells expressing Vps1-GFP and Abp1-mRFP (Fig. 1C, upper). As expected the Abp1-mRFP localisation was lost from sites, although Vps1 remained localised, demonstrating that its localisation was actin-independent. In the presence of Lat-A, Vps1 still colocalised with Sla1 (Fig. 1C, bottom) and its lifetime in patches was increased to 33.1±18.5 seconds (mean ± s.d.; *n*=102), which is a significant increase judged by an unpaired Student's *t*-test (*P*=0.0141). This Lat-A-dependent increase in Vps1 lifetime at endocytic sites adds further support to the idea that Vps1 is a bona fide endocytic protein. In addition, we quantified the number of stabilised endocytic patches formed under Lat-A treatment, which contained both Sla1 and Vps1. This gives an idea of the proportion of patches formed at the membrane that are able to recruit Vps1. In the presence of Lat-A, 78% of Sla1-mRFP patches also colocalised Vps1-GFP (*n*=102), supporting the idea that the majority of endocytic patches involve Vps1 function.

Deletion of Vps1 confers defects on endocytic machinery

Having established that Vps1 is in a position to function directly during endocytosis, we determined the effect that deletion of Vps1 has during single endocytic invagination events. The effect of *VPS1* deletion on the lifetime and behaviour of several proteins was investigated: Ent1 and Sla2, components of the endocytic coat complex; Las17, the yeast WASP homologue and activator of Arp2/3 mediated actin polymerisation; Abp1 and Sac6, components of the actin network that forms during invagination; and Rvs167, the amphiphysin proposed to be responsible for scission. As shown in Fig. 2A, lifetimes of five of the six proteins were markedly increased (see also supplementary material Movies 1 and 2).

To examine the behaviour of patches in more detail, kymographs were generated which depict movement of a patch over its lifetime. The endocytic coat proteins Sla2 and Ent1 localised longer at the plasma membrane before moving inwards (Fig. 2B). However, the movement inwards was often aberrant and patches could be seen to retract toward the plasma membrane (Fig. 2B, arrows). The WASP homologue las17 usually remains at the plasma membrane throughout invagination. In the *vps1*-deletion strain, movement in the plane of the membrane, as well as invagination and retraction could be observed. Normal and aberrant phenotypes were quantified

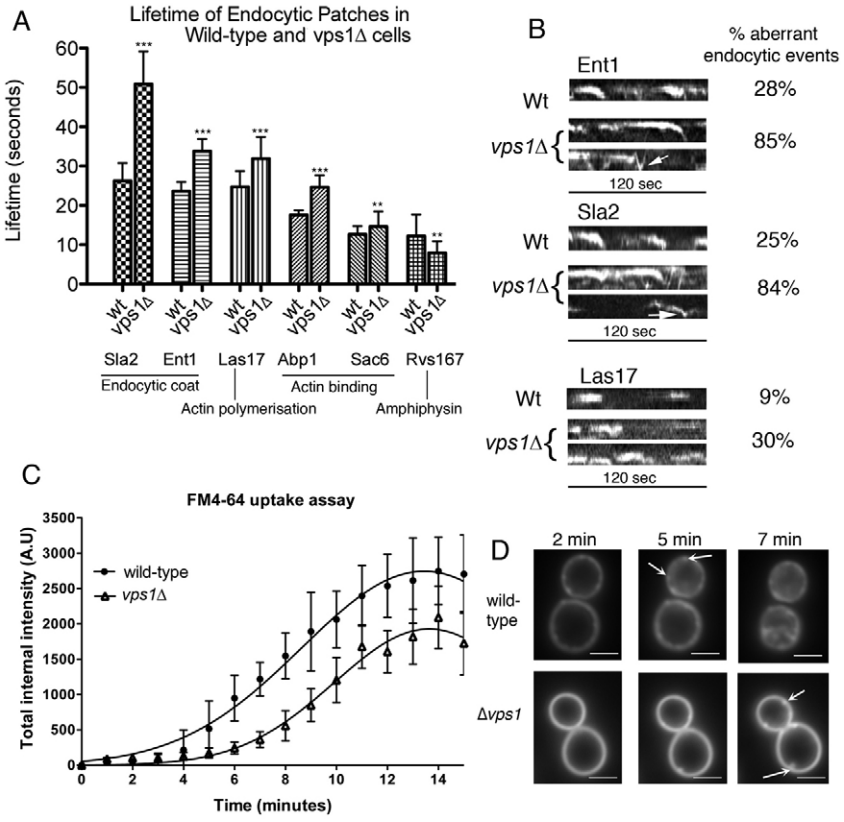

Fig. 2. The effect of *vps1* deletion on known endocytic proteins. (**A**) The lifetime of six endocytic proteins, Sla2, Ent1, Las17, Abp1, Sac6, and Rvs167 was analysed in the presence and absence of *vps1*. For wild-type cells, *n*=67, 22,119, 30, 60, 35 and for *vps1Δ* cells, *n*=19, 36, 121, 36, 69, 33 for the markers as ordered on graph. Error bars indicate s.d. ***$P<0.0001$ for Sla2, Ent1, Las17, Abp1; **$P<0.0004$ for Sac6 and 0.0002 for Rvs167. (**B**) Kymographs of Las17-GFP, Sla2-GFP and Ent1-GFP. Aberrant endocytic events for Sla2 and Ent1 were defined as those showing no invagination, movement in the membrane plane, delayed scission or retraction. For Las17, aberrant events were those showing movement in the membrane plane, inappropriate invagination and retraction. (**C**) FM4-64 internalisation was performed as described. Total internal cell fluorescence intensity (mean ± s.d.) was measured at each time point. (**D**) Representative images of wild-type and *vps1Δ* cells from three time points in the FM4-64-uptake assay. Arrows indicate foci of FM4-64 staining on the plasma membrane. Scale bars: 2 μm.

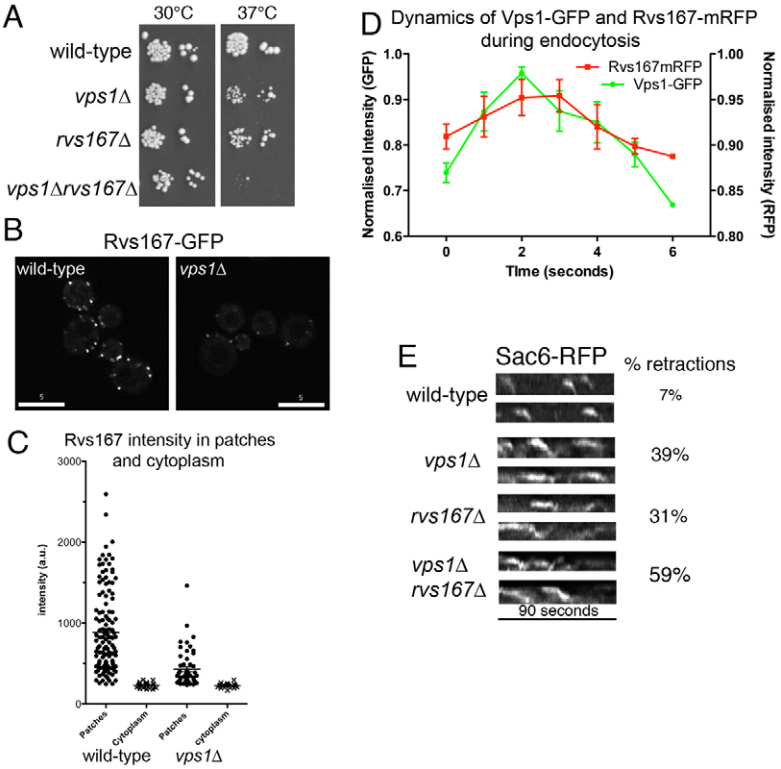

Fig. 3. The effect of *vps1* deletion on the amphiphysin Rvs167. (**A**) Strains carrying single deletions of either *vps1Δ* or *rvs167Δ* or a double-deletion strain were assessed for growth at 30°C and 37°C. (**B**) Rvs167-GFP localised in wild-type and *vps1Δ* cells. Images were recorded for 500 mseconds. Shown is a representative field of cells. Scale bars: 5 µm. (**C**) Fluorescence intensity of Rvs167-GFP patches and cytoplasmic background in wild-type and *vps1Δ* cells were recorded and plotted. Mean patch intensity: wild type, 885±508 units, *n*=128; vps1Δ, 429±227 units, *n*=53; *P*<0.0001. (**D**) Vps1-GFP was coexpressed with Rvs167-mRFP and intensity curves generated. Weighted averages of spot intensity were calculated and plotted. (**E**) Kymographs of Sac6-mRFP in wild-type, *vps1Δ*, *rvs167Δ* cells and in *vps1Δrvs167Δ* cells. Percentage of spots that retracted toward the membrane was counted. *n*=210, wild type; 46, *vps1Δ*; 52, *rvs167Δ*; 48, *vps1Δrvs167Δ* cells.

to determine the extent of the defect. Patches were analysed and classified according to their ability to invaginate and undergo scission normally. Deletion of *vps1* resulted in a severe disruption of these endocytic events (Fig. 2B).

Having shown that *vps1* deletion caused aberrant behaviour at the level of a single endocytic patch, we investigated the effect of *vps1* deletion in the whole cell. Although some studies have indicated no internalisation defects in cells lacking *vps1* expression (Geli and Riezman, 1998), others have demonstrated effects of *vps1* deletion on uptake of uracil permease (Fur4) activity (Yu and Cai, 2004). Deletion of many genes encoding proteins with accepted roles in endocytosis, such as Cap1, Scp1, Abp1, are reported to have no defect in several assays (Gheorghe et al., 2008; Huang et al., 1999; Kaksonen et al., 2005; Maldonado-Baez et al., 2008). However, the assays are often performed on fixed cells or over long time courses that do not detect more subtle, kinetic changes in uptake. To circumvent these issues, uptake of the lipophylic dye FM4-64 was performed under continuous observation following addition of dye to cells. Images were recorded over 15 minutes and total internal fluorescence intensity was measured (Fig. 2C). The plasma membrane was the first structure to be labelled following addition of FM4-64 (Fig. 2D). Foci of dye could then be seen in the plane of the plasma membrane before internal staining was observed (arrows). In wild-type cells, FM4-64 was seen next in endosomes and vacuoles. In *vps1Δ* cells, although plasma membrane staining occurred on the same time scale (1–2 minutes), the time for foci to form was slower. When the foci formed they persisted longer and there was a marked reduction in the rate at which internal fluorescence was observed. As expected from previous studies, the subsequent entry of FM4-64 to endosomes and the vacuoles was also delayed. Thus, *vps1* deletion affects internalisation of a bulk lipid marker, and the behaviour of single endocytic patches.

Overlapping roles of Vps1 and amphiphysin

The exception to the increased patch lifetime in *vps1Δ* cells (Fig. 2A) was the lifetime for the amphiphysin Rvs167. Furthermore, the retraction behaviour observed in kymographs for the various endocytic proteins (Fig. 2B) was reminiscent of the behaviour noted for *rvs167Δ* cells (Kaksonen et al., 2005). These data suggest that the function of Vps1 could be linked to, or overlap with, that of amphiphysins, as has been suggested from studies in mammalian cells (Ferguson et al., 2009; Itoh et al., 2005; Yamada et al., 2009). To investigate possible interplay between Vps1 and Rvs167, single deletion strains were crossed to determine any genetic interaction. Each deletion caused a slight temperature-sensitive growth phenotype (Fig. 3A). However, when combined, the mutations had a synergistic effect, and cells did not grow at 37°C. Such a phenotype is often suggested to indicate an overlapping role within a process (Tong et al., 2001).

Imaging of cells expressing Rvs167-GFP revealed an effect of *vps1* deletion on Rvs167-GFP localisation. In wild-type cells, Rvs167-GFP showed robust localisation to endocytic sites, whereas in *vps1Δ* cells, Rvs167 localised to endocytic sites, but its intensity was reduced (Fig. 3B). This effect was quantified by measuring fluorescence intensities of patches and cytoplasm in wild-type and *vps1Δ* cells. The intensity of patches was reduced by more than 50% in the mutant (*P*<0.0001, unpaired Student's *t*-test). In these strains, the overall level of Rvs167-GFP as determined by western blotting appeared to be similar, indicating that the reduced level of intensity is not due to degradation (data not shown). To determine whether Vps1 is involved in recruitment or stability of Rvs167 at the membrane Vps1-GFP and Rvs167-mRFP were coexpressed and localised. As shown in Fig. 3D, no time difference in localisation at the patch could be distinguished, indicating that Vps1 is more likely to be involved in stabilising Rvs167 at the endocytic site. The observation that the lifetimes of both tagged

proteins are reduced when coexpressed, further suggests that the presence of two bulky fluorophores compromises their close interactions within the patch.

To investigate the effect of deletion of *rvs167* and *vps1* on endocytosis, kymographs were generated in strains expressing the actin marker Sac6-RFP (Fig. 3E). This marker usually has a short lifetime with a sharp inward movement 1–2 seconds after arrival at the plasma membrane, followed by disassembly after scission. Defects were observed in all mutant strains, but those in the double mutant were most prevalent. Because retraction events have been quantified previously for cells lacking *rvs167*, we sought to compare this specific phenotype. Retraction events were defined as an endocytic event in which inward movement has taken place but in which scission does not occur and movement back towards the membrane is observed. As shown in Fig. 3C, retraction was seen in 31% of *rvs167Δ* endocytic events, which is similar to previously reported results (Kaksonen et al., 2005); in 39% of events in *vps1Δ* cells and in 59% of events in *rvs167Δvps1Δ* cells.

Invaginations do not form correctly in the absence of vps1

To investigate the function of Vps1 during invagination in more detail, an ultrastructural analysis using electron microscopy was performed. In this analysis, three main types of invagination at the plasma membrane were identified. These were defined as shallow (depth <40 nm) with the neck of the opening wide compared with the tubule diameter; pronounced (40–60 nm) when the neck of the tubule was the same or only slightly wider than the tubule diameter; deep (>60 nm), with the tubule neck about the same as the tubule diameter. In wild-type cells, 38% of invaginations fell in the pronounced category (Fig. 4A). Interestingly, in *vps1Δ* cells, the number of pronounced invaginations was significantly reduced to 24% (n=151 invaginations for wt and 91 for *vps1Δ*). During the analysis, it was noted that in wild-type cells, the majority of invaginations occurred perpendicular to the membrane whereas in *vps1Δ* cells, invaginations were often bent in appearance and the angle of invagination deviated from the perpendicular (Fig. 4B). This observation was quantified by measuring the angle of deviation of invaginations from a line drawn perpendicular to the membrane. As shown in Fig. 4C, there was a significant increase in the angle of invagination in the absence of *vps1*. The mean angle score for the wild type (8.93±9.24; mean ± s.d., n=54) was significantly lower than that in *vps1Δ* cells (18.55±12.66, n=54; P=0.0000169).

These data suggest that Vps1 functions to facilitate directed invagination leading to effective scission. This is supported by a model in which Vps1 forms a collar structure at the neck of an invaginating tubule in an analogous manner to dynamin in mammalian cells or in *shibire* mutant cells (Koenig and Ikeda, 1989). In this regard, a repeat structure can be detected on some of the deep invaginations seen in wild-type cells (Fig. 4D), but not in any deep or pronounced pits in *vps1Δ* cells.

Vps1 mutations reveal defects in endocytosis and endosomal trafficking

Previous work has shown a function for the N-terminal GTPase domain of Vps1 in intracellular membrane-trafficking events, but the role of its C-terminal domain has not been addressed. The mutants generated are depicted in Fig. 5A and were based on mutations in dynamin-1. Sequence alignment of dynamin-1 and Vps1 is shown in supplementary material Fig S1. The mutations have been reported to influence the GTPase activity, self assembly or other aspects of dynamin-1 function (Damke et al., 1994; Herskovits et al., 1993; Sever et al., 1999; Song et al., 2004a; Song et al., 2004b; Vater et al., 1992; Yu and Cai, 2004). Mutations, corresponding positions in human dynamin-1 and temperature sensitivity of the *vps1Δ* cells transformed with plasmids carrying the mutations are listed in Table 1.

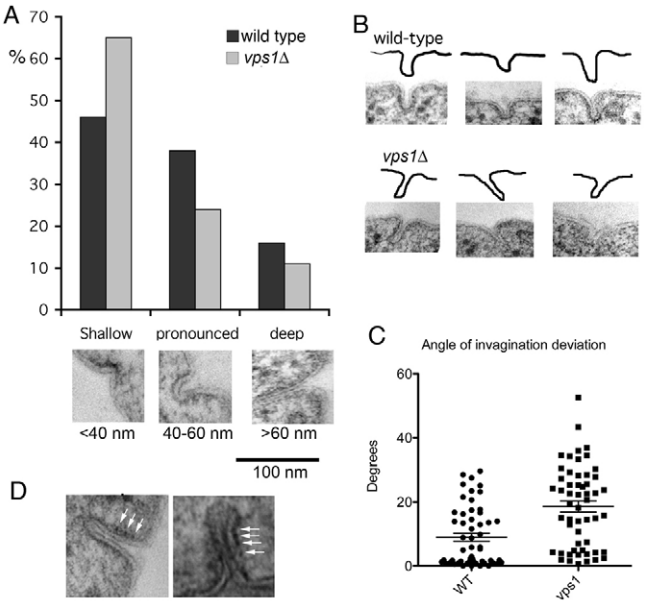

Fig. 4. Ultrastructural analysis of endocytic patches in *vps1Δ* cells. (**A**) The proportion of shallow, pronounced and deep invaginations in wild-type and *vps1Δ* cells was counted (n=151, wild type; n=91, *vps1Δ*). (**B**) Images of pronounced invaginations in cells in the presence and absence of Vps1. Above the micrographs are outline tracings showing the invagination profile. (**C**) The angle of invagination relative to a line perpendicular to the plasma membrane was measured for both wild-type and *vps1Δ* invaginations. Horizontal lines indicate the means ± s.d. (**D**) In pronounced invaginations in wild-type cells, a repeated structure at the side of the invaginations can be observed in sections (arrows).

The first analysis of the mutants used a recently published assay for endocytic recycling, in which a reporter construct, containing the SNARE protein Snc1 fused to both an invertase activity at its N-terminus and GFP at its C-terminus, is transformed into *vps1Δ* cells (Burston et al., 2009). This assay allows differentiation between endosomal trafficking and endocytic internalisation defects. If Vps1 function is predominantly intracellular, for example

Table 1. Mutations generated in Vps1 and corresponding positions in dynamin-1

Human dynamin-1	Yeast Vps1	Temperature sensitive in yeast?	Ref.
S45N	S43N	+	(Marks et al., 2001)
T65A	T63A	+	(Song et al., 2004a)
R66C	R64C	+	(Marks et al., 2001)
T141Q	T183Q	+	(Song et al., 2004a)
G146S *shibire* ts2	G188S	+	(Narayanan et al., 2005)
G273D *shibire* ts1	G315D	+	(Damke et al., 1995)
I690K	I649K	+	(Song et al., 2004b)
K694A	K653A	–	(Song et al., 2004b)
R725A	R684A	–	(Sever et al., 1999)
K730A	K689A	±	(Sever et al., 1999)

in endosomal fusion–fission events, then its loss will result in the accumulation of fused Snc1 and invertase inside cells, so that when cells are incubated with appropriate substrate, colonies will be white. If the primary function of the protein is in endocytic internalisation, then uptake of the SNARE will be delayed, more invertase will be exposed at the surface and in the assay colonies will appear dark brown. In wild-type cells, there was continuous cycling of Snc1, and the cells appeared light brown when assayed. Cells in which *vps1* was deleted were transformed with an empty plasmid or with plasmids carrying wild-type or mutant *vps1*. In the assay, there was a clear outcome, with *vps1Δ* colonies remaining largely white (Fig. 5B). Those cells expressing wild-type *VPS1* restored trafficking, such that the expected light-brown colouring was observed. The mutants fell into three classes. Those that lie in the N-terminal half caused a phenotype that was similar to *vps1Δ*, indicating the importance of the GTPase function in endosomal trafficking or recycling. Most of the mutants in the C-terminal domain were similar to the wild type, suggesting that C-terminal functions are less important for endosomal recycling. However, the mutant I649K was darker than the wild type, indicating a more predominant endocytic phenotype.

Two mutants were analysed further. These were the mutants T63A (representative of GTPase function) and I649K (from the GTPase effector or self-assembly domain). Three assays were used to report on the functional contribution of the N- and C-terminal domains in intracellular trafficking events. First, the localisation of the GFP fusion in the invertase–Snc1 reporter was examined in wild-type and mutant strains (Fig. 5C; *n*=100 cells for plasma membrane staining counts). In wild-type cells, or cells in which *VPS1* was re-expressed in the null strain, GFP localised to the plasma membrane in 93% of cells and to large internal organelles (probably endosomes) but there was relatively little background signal from small vesicles. In *vps1Δ* cells, the majority of GFP appeared to localise to small vesicles with less in larger organelles and only 13% of cells had plasma membrane staining, indicating an endosomal trafficking defect. Expression of the T63A GTPase mutant was similar to the null phenotype, with predominantly small vesicles and a few endosomes (8% cells had plasma membrane staining). The mutant in the C-terminal region (I649K) had a predominantly plasma membrane and endosomal localisation (87% cells had plasma membrane staining). Therefore, the GTPase domain is crucial for endosomal recycling.

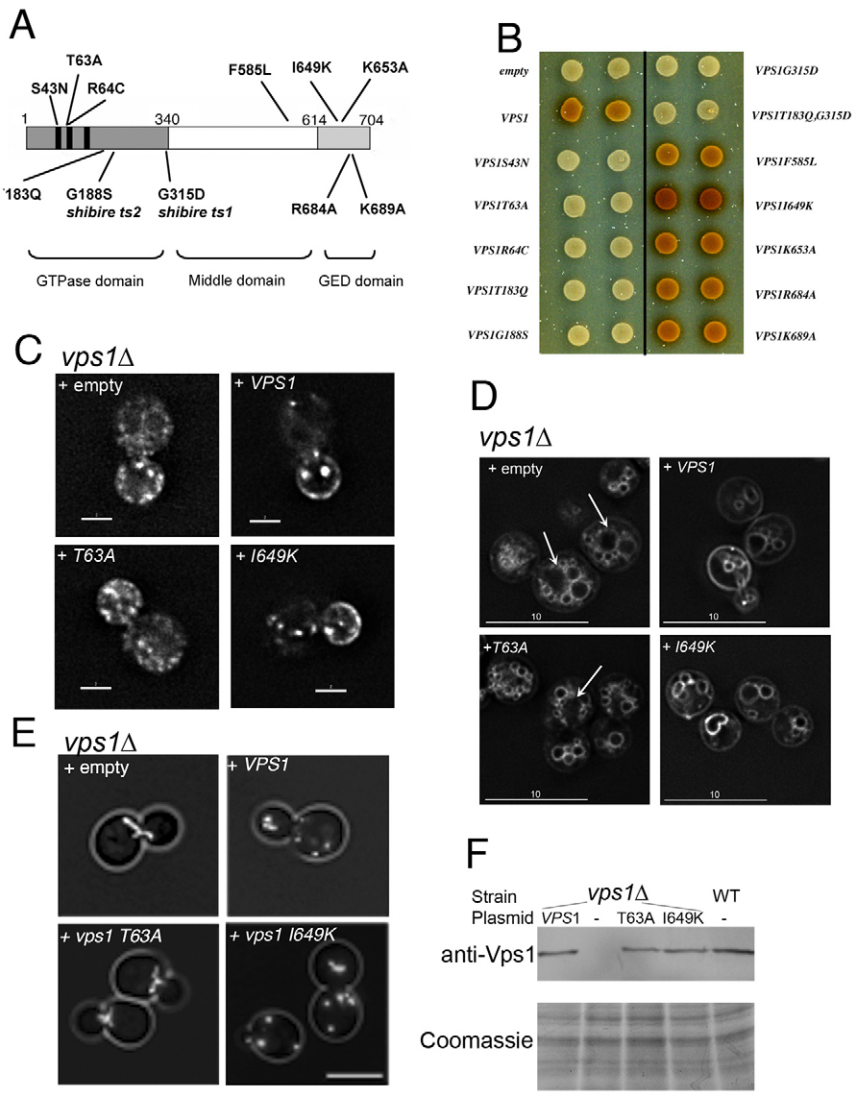

Fig. 5. Analysis of the endosome, vacuole and peroxisome in Vps1 mutants. (**A**) Mutations were generated in Vps1 as depicted. (**B**) Cells deleted for *vps1* were transformed with a construct expressing the recycling SNARE protein Snc1, fused to *SUC2* and GFP. Localisation of invertase is detected in a colorimetric assay. (**C**) Localisation of GFP-Snc1-SUC2 construct was analysed in wild-type, *vps1Δ*, T63A and I649K mutants. Scale bars: 2 µm. (**D**) Uptake of FM4-64 reveals vacuolar trafficking defects in a subset of *vps1* mutant strains. Cells were incubated for 10 minutes with FM4-64, washed and then visualised after 90 minutes. Arrows indicate clusters of endosomes or fragmented vacuoles surrounding a large weakly stained vacuole, the class F phenotype. Scale bars: 10 µm. (**E**) Peroxisomes labelled with GFP peroxisome reporter were visualised in a *vps1Δdnm1Δ* strain expressing plasmids with mutant versions of *vps1*. Images are compressed *Z*-stacks for fission-proficient strains and in a single plane for fission-deficient strains. Scale bar: 5 µm. (**F**) Whole-cell extracts separated by SDS–PAGE. The upper part of gel was used for western blotting with mouse anti-Vps1 polyclonal antibody. The lower half of the gel was removed and stained with Coomassie Blue to indicate protein-loading levels.

Defects in trafficking to the vacuole were also shown by FM4-64 staining (Fig. 5D). *vps1Δ* cells have been classed as class F vacuolar mutants and they have a rather heterogeneous phenotype, with both fragmented vacuoles and vacuoles with aberrant morphologies (Raymond et al., 1992). A common feature of these cells is a weakly stained vacuole with clusters of vacuoles around it. In cells expressing *VPS1*, uptake of FM4-64 showed clear localisation to vacuolar membranes (Fig. 5D). In *vps1Δ*, there was a lower level of vacuolar localisation and a high level of staining, especially of clustered endosomes around the vacuole (Fig. 5D, arrows). The GTPase-domain mutant T63A was phenotypically similar to the *vps1Δ* strain. The C-terminal mutation I649K showed clear vacuolar membrane staining that was similar to the wild type, indicating relatively normal trafficking.

Finally, we addressed whether the Vps1 mutants would rescue the characteristic phenotype of peroxisomes in *vps1Δdnm1Δ* cells in which only one large peroxisome is observed when using a peroxisomal reporter GFP (Motley and Hettema, 2007). In support of the idea that the GTPase activity functions to drive membrane fusion–fission reactions, the mutant affecting this part of the protein was also defective in peroxisomal fission. Again, the I649K mutant in the C-terminal region of the protein was able to rescue the peroxisome defect and restore the normal number of peroxisomes in cells (Fig. 5E). To verify that the effects observed in the assays were not due to absence of protein as a result of instability and degradation, protein extracts were made from wild-type cells and from *vps1Δ* cells carrying *VPS1*, T63A, I649K and empty plasmids. The level of Vps1 protein expressed was comparable in all strains, apart from the null (Fig. 5F).

Overall, these data demonstrate the importance of the GTPase domain in known Vps1 functions in endosomal and vacuolar trafficking and peroxisome morphology. By contrast, the I649K C-terminal mutation conferred an endocytic phenotype in the invertase assay, but mutants were similar to the wild type for peroxisomal and vacuolar-trafficking assays. To investigate the endocytic phenotype further, the behaviour of key endocytic proteins was analysed in the T63A and I649K Vps1 mutants and compared with that in wild-type and *vps1Δ* cells. When these *vps1* mutants were expressed in Las17-GFP cells, they showed a lifetime that was not statistically different from the *vps1*-null strain (Fig. 6A, supplementary material Movie 1), suggesting that during endocytosis, both N- and C-terminal domains are necessary for function. Kymographs also showed the increase in lifetime. Furthermore, although the majority of patches simply showed an increase in the time spent in the plane of the plasma membrane, a small proportion of patches (≤20%) in *vps1Δ* cells expressing either an empty plasmid or mutant plasmids, showed aberrant inward movements (Fig. 6B).

Analysis of Sla2GFP patch lifetimes also revealed defects in the Vps1 mutant lifetimes and behaviour, although interestingly, none of the mutants had a lifetime defect as severe as that in the null (Fig. 6C). Again, there were no significant differences in lifetimes between Vps1 T63A and I649K mutants. Kymographs and movies show that both mutants had aberrant invaginations and retractions (Fig. 6D; supplementary material Movie 2). Finally, the effect of Vps1 mutation on Rvs167 behaviour was investigated. Re-expression of wild-type *VPS1* fully rescued the shortened lifetime of Rvs167 in the *vps1*-null strain (Fig. 6E,F). In addition, both T63A and I649K mutants showed weaker localisation to the patches and reduced patch lifetimes, similar to the null strain.

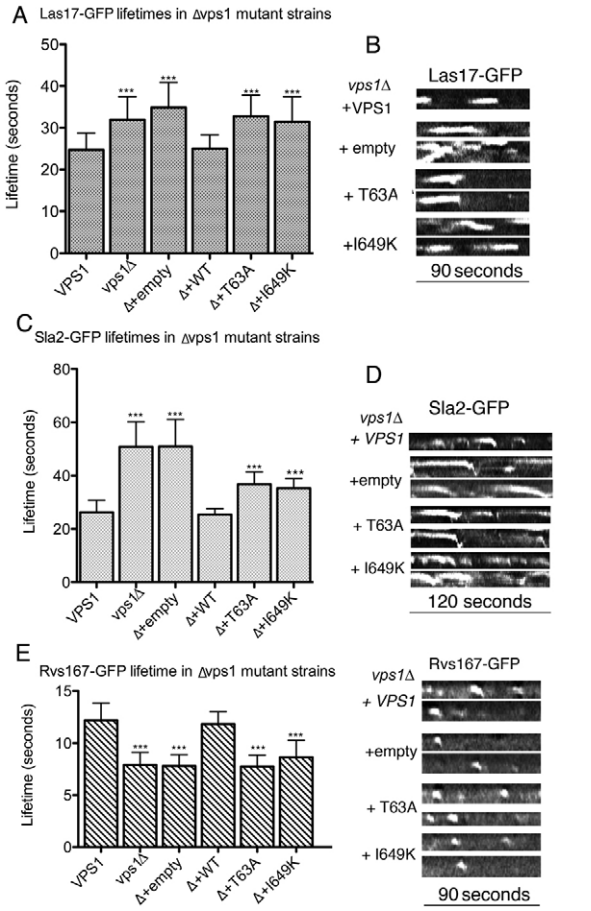

Fig. 6. Vps1 mutants show defects in the behaviour of endocytic proteins. (**A**) Lifetime of Las17-GFP was measured in wild-type and *vps1Δ* cells, and in *vps1Δ* strains transformed with plasmids (empty, *VPS1*, *vps1T63A* and *Vps1I649K*). *n*=119, 121, 24, 34, 41, 25, respectively. Error bars indicate s.d. All mutant *vps1* lifetimes are significantly different from the wild type (***P<0.0001). (**B**) Kymographs of Las17-GFP in the strains. (**C**) Lifetime of Sla2-GFP was measured in wild-type and *vps1Δ* cells and in *vps1Δ* strains transformed with the plasmids as indicated. *n*=67, 24, 24, 35, 40, 23, respectively. Error bars indicate s.d. All mutants are significantly different from the wild-type and null strains (***P<0.0001). (**D**) Kymographs of Sla2-GFP in each of these mutants. Exposure time was increased to allow visualisation of spots in the mutant and null strains. (**E**) Lifetime of Rvs167-GFP in wild-type and *vps1Δ* cells and in *vps1Δ* strains transformed with the plasmids as indicated. *n*=35, 33, 116, 91, 114, 108, respectively. Error bars indicate s.d. All mutants are significantly different from wild type (***P<0.0001).

Wild-type Vps1 tubulates membranes in vitro

The electron microscopy data suggested that Vps1 acts to facilitate the shallow-to-pronounced invagination structure in vivo and/or to ensure directed inward growth of the invaginating tubule. We then aimed to determine whether purified Vps1 has the capacity to bind to and possibly tubulate membranes in vitro. This would add support to the idea of Vps1 performing this key role directly in vivo, rather than through recruitment of other activities. Vps1 was purified as described, and incubated with liposomes (+GTP). Binding to liposomes was assessed by centrifugation of membranes. As shown in Fig. 7A, Vps1 pelleted in the presence of liposomes (upper panel), but not in their absence (lower panel),

demonstrating the ability of Vps1 to bind liposomes. Next, the effect on liposome structure was investigated. Vps1 was incubated with liposomes and GTPγs and applied to EM grids. As shown in Fig. 7B, the presence of Vps1 had a marked effect on liposome structure, with tubules decorated with Vps1 clearly visible after incubation. These tubules were also formed at a ten-times lower concentration of Vps1 (supplementary material Fig. S2). Finally, we addressed whether self-assembly of Vps1 has a role in its ability to tubulate membranes. The mutation I649K corresponds to the I690K mutation in human dynamin and this mutation has been shown to affect oligomerisation of dynamin (Song et al., 2004b). I649K Vps1 was purified, and tested for its ability to oligomerise in the presence of GTPγs in a centrifugation-based assay. In contrast to the lipid-binding assay, which was performed in the presence of GTP, use of GTPγs stabilises self assembly of Vps1. Fig. 7C shows that although Vps1 could self assemble, allowing it to pellet under the conditions described, I649K Vps1 did not pellet, confirming the oligomerisation defect in this mutant. Mutant Vps1 was, however, able to bind liposomes (Fig. 7A). Analysis by EM reveals that Vps1 I649K did not tubulate membranes (Fig. 7B), demonstrating the importance of self-assembly in the tubulation process. EM analysis of wild-type Vps1 in the presence of GTPγs but without liposomes showed no tubules (supplementary material Fig. S2), confirming that tubules are liposome dependent.

Discussion

Dynamin is considered to be a central protein in endocytosis in metazoan cells, and the absence of this role in yeast has raised many questions (see Ferguson et al., 2009; Geli and Riezman, 1998; Robertson et al., 2009). Here, we present data that we believe strongly support a role for the dynamin-like protein Vps1 in the endocytic process in *Saccharomyces cerevisiae*. Additional evidence for Vps1 function in endocytosis has also been recently reported by Nannapaneni and colleagues (Nannapaneni et al., 2010).

Given our findings, it seems somewhat surprising that such an endocytic defect was not previously reported. We think that there are several reasons for this, including the promiscuous nature of Vps1 function in several other membrane-trafficking steps and also because deletion of *vps1* does not show obvious defects in uptake of commonly used reporters such as Lucifer Yellow (Geli and Riezman, 1998). Lack of clear defects in these classical endocytic assays is not, however, uncommon, with deletion of many endocytic genes causing no apparent defects. In terms of a role for Vps1 in endocytosis, critically, we show the Vps1 colocalises with other endocytic proteins (Fig. 1A), and second that the *vps1* deletion strain has clear defects in behaviour of endocytic reporter proteins and a kinetic defect in uptake of the dye FM4-64 (Fig. 2). Three questions were then addressed: (1) When does Vps1 function during endocytosis? (2) How does it function? (3) What are the roles of its N- and C-terminal domains in this function?

To ascertain when Vps1 functions during endocytosis, the cortical lifetime of Vps1 was measured and found to be 8.7 seconds. This is short compared with many other endocytic proteins such as Sla1 (~25–30 seconds and Abp1 ~15–18 seconds), but more similar to timing of Myo3 and Myo5 (~10–12 seconds), the actin-binding protein Sac6 (10–12 seconds) and the amphiphysins (~ 9–10 seconds) (Gheorghe et al., 2008; Jonsdottir and Li, 2004; Kaksonen et al., 2003; Kaksonen et al., 2005). Timing of its arrival at the membrane, about 5 seconds after Abp1, indicate that it is not

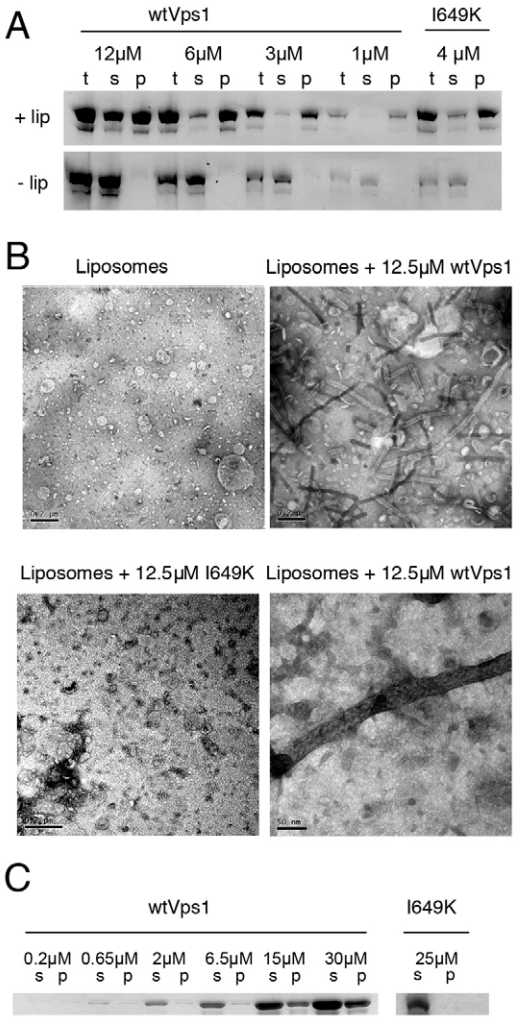

Fig. 7. Vps1 binds and tubulates liposomes. (**A**) Vps1 was incubated with liposomes, which were then subjected to centrifugation and total protein (t), pellets (p) and supernatants (s) were analysed by SDS–PAGE. Varying concentrations of wtVps1, or 4 μM I649K Vps1 were used in the presence (top panel) or absence (bottom panel) of liposomes. (**B**) Liposomes were analysed using electron microscopy in the presence and absence of wt Vps1 or I649K Vps1. A high-resolution image of a tubulated liposome reveals a regular organisation of negative staining along the formed tubule. (**C**) Self-assembly assays of wt Vps1 and I649K Vps1 were performed as described. s, supernatant; p, pellet fractions.

functioning in recruitment of endocytic coat or early acting F-actin polymerisation factors and most likely has a role at the onset or during the invagination step of endocytosis. This appears to be, at least qualitatively, similar to the situation in Swiss-3T3 cells in which dynamin fluorescence increased sharply and transiently at clathrin-labelled spots just before inward movement (Merrifield et al., 2002).

The question of the mechanism of function then arises. The behaviour of several endocytic proteins was studied in *vps1Δ* cells. Of these, one had a reduced level of localisation and a shorter lifetime in patches (Figs 2, 3). This was the amphiphysin protein Rvs167. However, in colocalisation studies, we were not able to distinguish arrival times to patches, indicating that Vps1 is more likely to maintain Rvs167 at the membrane rather than

recruit it (Fig. 3D). There is currently no evidence that Vps1 interacts directly with Rvs167. However, there are clear links between the proteins. One candidate for linking Vps1 and Rvs167 function is Sla1, which has reported interactions with both proteins (Stamenova et al., 2004; Yu and Cai, 2004). Alternatively, Vps1 might induce changes to the membrane itself that favour stable binding of Rvs167. From the ultrastructural analysis (Fig. 4), one potential role for Vps1 is in the switch from a shallow wide-necked pit to a parallel-sided invaginating tubule. The in vitro data (Fig. 7) also demonstrated that Vps1 has the capacity to bind to liposomes and to tubulate them. Taken together, we suggest a model in which Vps1 is recruited to membranes in an actin-independent manner, but after F-actin polymerisation has been initiated. As rapid actin polymerisation drives inward membrane growth, Vps1 potentially in concert with Rvs167, could bind to the membrane and form an oligomerised structure to bring the sides of the tubule essentially parallel. This action would ensure that the force from actin polymerisation is driving directly into the cell around the tubule. If a parallel-sided tubule is not formed, directed inward movement would be less likely, explaining why angles of invagination are more varied in the *vps1Δ* strain. Such disorganised forces might also be expected to cause the more erratic patch behaviour that is observed. The idea of a sheath of protein along the invaginated tubule region had been suggested in endocytic modelling studies (Liu et al., 2009). This protein sheath is proposed to act as a filter to effect a separation of lipid species and thus generate lipid phase boundary forces, which, in concert with the force from actin polymerisation, could be responsible for membrane scission. Liu and colleagues propose that this sheath is entirely composed of amphiphysin (Liu et al., 2009). Our data suggest that it could be initiated or maintained by the function of Vps1.

Finally, the role of distinct domains within Vps1 was investigated. Ten mutant forms of Vps1 were generated and expressed. The sites and amino acid changes made were based on mutations previously generated in mammalian dynamin or from the original *Drosophila shibire* mutations. The effects of two of these mutations T63A and I649K, which correspond to dominant-negative mutations in mammalian cells, were investigated. Taken together, the data indicate that the N-terminal GTPase domain of Vps1 is crucial for its function in endosomal recycling, vacuolar uptake of FM4-64 and in peroxisomal fission. Interestingly, mutations in the C-terminal domain did not compromise the function of Vps1 in these assays. The effect of Vps1 mutations in endocytosis was, however, markedly different. Not only does the GTPase domain have an important role in successful invagination, but the C-terminal region is also involved. For all endocytic markers studied, the I649K mutation in the C-terminal region caused effects as severe as those in the GTPase region. Biochemical studies (Fig. 7) reveal that I649K mutation in the C-terminal domain of Vps1 prevents self-assembly. Thus, self-assembly is important for endocytic function of Vps1, but does not appear to be required for the other trafficking roles investigated. This is a key result that defines the role of the yeast dynamin during endocytosis compared with its other roles in cell-membrane trafficking.

Materials and Methods

Materials

Unless stated otherwise, chemicals were obtained from Sigma. Media were from Melford Laboratories (Ipswich, Suffolk, UK) (yeast extract, peptone, agar) or Sigma (minimal synthetic medium and amino acids). Lat-A and FM4-64 were from Molecular Probes.

Yeast strains and cell growth

Yeast strains used in this study are listed in supplementary material Table S1. Vps1 was deleted with a PCR-based recombination approach (Longtine et al., 1998) using a *Candida glabrata LEU2* marker. Deletion was verified by colony PCR. pHB4 was integrated into the *vps1Δ* strain (KAY1095) to generated a strain expressing the reporter GFP-*SNC1*-*SUC2*. All strains carrying GFP or mRFP tags have growth properties that are similar to control strains when expressed singly. The combination of Vps1-GFP and Rvs167-mRFP appears to cause some instability and both have reduced patch lifetimes. Vps1-GFP was a gift from Andreas Mayer (University of Lausanne, Lausanne, Switzerland) and was previously characterised (Peters et al., 2004). Cells were grown with rotary shaking at 30°C in liquid YPD medium (1% yeast extract, 2% Bacto-peptone, 2% glucose supplemented with 40 μg/ml adenine) or in synthetic medium (0.67% yeast nitrogen base, 2% glucose) with supplements. Transformations were performed using lithium acetate as described (Kaiser et al., 1994). The plate-based invertase assay was performed as described (Burston et al., 2009).

Generation of Vps1 plasmid and mutations

Plasmids used in this study are listed in supplementary material Table S2. Sequence encoding *VPS1* and 320 bp upstream was cloned from genomic DNA and cloned into a plasmid pEH318 marked with *URA3* to generate plasmid pKA677. Mutations were generated using site-directed mutagenesis kits (Stratagene). Mutations generated are listed in Table 1. All constructs were verified by sequencing. The mutation F585L arose spontaneously in the PCR process and this mutation was included for analysis alongside the others.

Vps1 purification

Vps1 cloned in pCRT7/Nt-TOPO was a gift from Andreas Mayer (University of Lausanne, Lausanne, Switzerland). His-tagged Vps1 was expressed in C43 cells [Lucigen Overexpress^{TM} C43(DE3) SOLOs] by induction with 1 mM IPTG for 7 hours at 37°C. Pelleted cells from 2 litres of culture were resuspended in buffer (30 mM imidazole, 10 mM Na_2HPO_4, 10 mM NaH_2PO_4, 500 mM NaCl, pH 7.4), and the protein was purified using HisTrap HP nickel columns (GE Healthcare). Vps1 was concentrated and buffer exchanged in a centrifugal filter device (Centriprep, Millipore) into PBS. Approximately 2 mg protein was obtained from 2 litres of cell culture. I649K protein was expressed in C43 cells and induced at room temperature for 48 hours before being harvested and purified as for wild-type Vps1.

Liposome preparation

For preparation of liposomes, 11 μl of a 25 mg/ml solution of Folch fraction 1 (Sigma) was dried under nitrogen, then resuspended in 200 μl buffer B (20 mM HEPES pH 7.2, 100 mM KCl, 2 mM $MgCl_2$, 1 mM DTT) at 60°C for 30 minutes with gentle agitation. Liposomes were extruded 11 times through polycarbonate filters with 1.0 μm pores. Self-assembly assays were carried out using an adapted method (Yoon et al., 2001). Vps1 was added to liposome buffer at the concentrations shown and centrifuged at 313,000 ***g*** for 15 minutes to remove any aggregated protein. GTPγS was added to 0.5 mM, and oligomerised protein was pelleted by centrifugation at 250,000 ***g*** for 15 minutes; supernatants and pellets were analysed by SDS–PAGE. Vps1 (pre-spun at 313,000 ***g*** for 15 minutes) was mixed with 20 μl liposomes in the presence of 2 mM GTP, 2 mM $CaCl_2$, 2 mM $MgCl_2$ and 2 mM DTT, and incubated at room temperature for 30 minutes to measure liposome binding. Liposomes and bound protein was pelleted by centrifugation at 250,000 ***g*** for 15 minutes, and samples analysed by SDS–PAGE. Vps1 (12.5 μM) was mixed with liposomes (0.5 mg/ml) and GTPγS (0.5 mM) and incubated for 30 minutes at room temperature to measure in vitro liposome tubulation. GTPγS was not essential, but enhanced self-assembly. The resulting mixture was then processed for electron microscopy.

Electron microscopy

In vitro tubulation was visualised by negative staining. Samples were adsorbed on glow-discharged carbon-coated copper grids and stained with 0.75% uranyl formate. Electron micrographs were recorded on a Philips CM100 electron microscope using a Gatan MultiScan 794 CCD camera.

Fluorescence microscopy

Epifluorescence microscopy was performed using either of the following two systems: Olympus IX-81 inverted microscope with a DeltaVision RT Restoration Microscopy System using a 100×/1.40 NA oil objective, Photometrics Coolsnap HQ camera with Imaging and Image capture performed using SoftWoRx^{TM} image analysis and model-building application (Applied Precision Instruments, Seattle); or, with an Olympus IX-81 inverted microscope using MAG Biosystems acquisition software version 7.5.2.0 (by Metamorph) with a Photometrics CoolsnapHQ^2 Turbo 1394 camera. 3D deconvolution was carried out with Autoquant X AutoDeblur Gold WF version X2.1.3. Post-acquisition image viewing, analysis and optimisation was carried out using Image-Pro Analyser version 6.3 (both by Media Cybernetics). A 150×/1.45 oil objective was used for acquiring time-lapse images and a 60×/1.25 oil objective for FM4-64 experiments. All experiments were carried out at room temperature (22°C). TIRF microscopy was performed on an inverted Laser TIRF3 Imaging system (Carl Zeiss) with excitation lasers set to 488 nm and 561 nm to

visualise GFP- and mRFP-tagged proteins. Acquisition was performed using an alpha plan-Apochromat 100×/1.46 NA oil objective and PVCAM camera. Imaging and Image capture was performed using AxioVision Rel 4.7 software at 20°C.

For analysis of Vps1-GFP colocalisation at patches with Abp1mRFP, only fully overlapping profiles were considered (as shown in supplementary material Fig. S3). This was done to avoid consideration of endosomally localised Vps1, which can localise in spots close to endocytic patches.

For uptake of FM4-64 (Fig. 2), 40 µl of log-phase cells were pipetted into a well of a µ-slide VI-flat slide (IBIDI). 40 µl of 32 µM FM4-64 (Invitrogen) were added to the well corresponding to the same channel and cells were visualised at 591 nm (Texas Red filter). Images were taken for 25 minutes at 10 second intervals. Analysis of intensity/unit area was carried out using Image-Pro Analyser (version 6.3.0.512). For uptake of FM4-64 (Fig. 5); 0.25 µl of 16 mM FM4-64 was added to 500 µl culture for 10 minutes. Cells were washed and were viewed after 90 minutes. Peroxisomes were labelled with the peroxisome lumenal marker GFP- PTS1, a GFP fusion to a peroxisome targeting signal type I under control of the Tpi1 promoter and visualised and imaged as previously described (Motley and Hettema, 2007).

For live-cell imaging, cells expressing tagged proteins were visualised after growing to early log phase in synthetic medium with appropriate supplements. 2.8 µl of culture grown in synthetic medium was applied to an uncoated slide and covered before inverting for imaging. Unless stated otherwise, time-lapse live-cell imaging of GFP-tagged proteins was performed with 1 second time lapse. All image data sets were deconvolved, the distance of moving fluorescence spots were measured, and the arbitrary profile of intensity values, image coordinates and tracking of patch movements were established using the SoftWoRx application. Images were exported as TIFF files and image size adjusted to 300 d.p.i. and assembled using Adobe Photoshop CS2. Kymographs were assembled using ImageJ software. Statistical analysis of lifetimes was performed using Graphpad Prism software.

Preparation of yeast for electron microscopy

50 ml of mid log phase yeast growing in YPD medium (1% yeast extract, 2% peptone, 2% dextrose) was concentrated by syringe filtering, transferred to a Leica flat specimen carrier and frozen in a Leica EMPACT high pressure freezer. Freeze substitution and fixation were carried out in a Leica AFS freeze substitution unit. Frozen specimens were transferred into fixative (0.1% uranyl acetate, 2.5% glutaraldehyde, 5% H_2O in acetone) at –90°C for 48 hours, then warmed to –25°C for 12 hours, followed by three 15-minute washes in pure acetone at –25°C. They were infiltrated with 1:2 mix of Lowicryl HM 20 (Polysciences):acetone for 1 hour at –25°C, 1:1 Lowicryl:acetone for 1 hour at –25°C, 2:1 Lowicryl:acetone for 1 hour at –25°C and 100% Lowicryl overnight at –25°C. Samples were placed in fresh 100% Lowicryl at –25°C and polymerised with the UV lamp for 48 hours, warmed up to +25°C over 10 hours and incubated for 24 hours with the UV lamp. 20- to 60-nm-thick sections were cut using a Diatome Ultrasonic diamond knife on a Leica EM UC6 ultramicrotome (Leica Microsystems), stained with 1% aqueous uranyl acetate for 10 minutes, washed 20 times with water and stained with Reynold's lead citrate for 10 minutes, washed again and air dried. They were viewed at 100 kV in a Hitachi H7600 TEM.

We would like to thank Liz Smythe (University of Sheffield) for critical reading of the manuscript; Rosaria Costa, Wesley Booth, and Jackie Price for technical assistance; Andreas Mayer (University of Lausanne, Switzerland) for the His-Vps1 plasmid and the Vps1GFP expressing yeast strain, Dave Drubin (University of California, Berkeley) for yeast strains and Liz Conibear (University of British Columbia, Vancouver) for the GFP-Snc1-SUC2 construct. The work was supported by a MRC Senior non-clinical fellowship to K.R.A. (G0601600) and BBSRC grant (BB/G011001/1); a BBSRC studentship to S.A. and a Wellcome Trust Senior Fellowship to E.H.H. (WT084265). The light microscopy-imaging centre at the University of Sheffield was funded by a grant from the Wellcome Trust (GR077544AIA). Deposited in PMC for release after 6 months.

Supplementary material available online at
http://jcs.biologists.org/cgi/content/full/123/20/3496/DC1

References

Ayscough, K. R., Stryker, J., Pokala, N., Sanders, M., Crews, P. and Drubin, D. G. (1997). High rates of actin filament turnover in budding yeast and roles for actin in establishment and maintenance of cell polarity revealed using the actin inhibitor latrunculin-A. *J. Cell Biol.* **137**, 399-416.

Burston, H. E., Maldonado-Baez, L., Davey, M., Montpetit, B., Schluter, C., Wendland, B. and Conibear, E. (2009). Regulators of yeast endocytosis identified by systematic quantitative analysis. *J. Cell Biol.* **185**, 1097-1110.

Cao, H., Orth, J. D., Chen, J., Weller, S. G., Heuser, J. E. and McNiven, M. A. (2003). Cortactin is a component of clathrin-coated pits and participates in receptor-mediated endocytosis. *Mol. Cell. Biol.* **23**, 2162-2170.

Cao, H., Weller, S., Orth, J. D., Chen, J., Huang, B., Chen, J. L., Stamnes, M. and McNiven, M. A. (2005). Actin and Arf1-dependent recruitment of a cortactin-dynamin complex to the Golgi regulates post-Golgi transport. *Nat. Cell Biol.* **7**, 483-492.

Cerveny, K. L., Tamura, Y., Zhang, Z., Jensen, R. E. and Sesaki, H. (2007). Regulation of mitochondrial fusion and division. *Trends Cell Biol.* **17**, 563-569.

Chen, M. S., Obar, R. A., Schroeder, C. C., Austin, T. W., Poodry, C. A., Wadsworth, S. C. and Vallee, R. B. (1991). Multiple forms of dynamin are encoded by shibire, a drosophila gene involved in endocytosis. *Nature* **351**, 583-586.

Damke, H., Baba, T., Warnock, D. E. and Schmid, S. L. (1994). Induction of mutant dynamin specifically blocks endocytic coated vesicle formation. *J. Cell Biol.* **127**, 915-934.

Damke, H., Baba, T., Vanderbliek, A. M. and Schmid, S. L. (1995). Clathrin-independent pinocytosis is induced in cells overexpressing a temperature-sensitive mutant of dynamin. *J. Cell Biol.* **131**, 69-80.

Dawson, J. C., Legg, J. A. and Machesky, L. M. (2006). Bar domain proteins: a role in tubulation, scission and actin assembly in clathrin-mediated endocytosis. *Trends Cell Biol.* **16**, 493-498.

Doyle, T. and Botstein, D. (1996). Movement of yeast cortical actin cytoskeleton visualized *in vivo*. *Proc. Natl Acad. Sci. USA* **93**, 3886-3891.

Ferguson, S., Raimondi, A., Paradise, S., Shen, H. Y., Mesaki, K., Ferguson, A., Destaing, O., Ko, G., Takasaki, J., Cremona, O. et al. (2009). Coordinated actions of actin and BAR proteins upstream of dynamin at endocytic clathrin-coated pits. *Dev. Cell* **17**, 811-822.

Gammie, A. E., Kurihara, L. J., Vallee, R. B. and Rose, M. D. (1995). Dnm1, a dynamin-related gene, participates in endosomal trafficking in yeast. *J. Cell Biol.* **130**, 553-566.

Geli, M. I. and Riezman, H. (1998). Endocytic internalization in yeast and animal cells: similar and different. *J. Cell Sci.* **111**, 1031-1037.

Gheorghe, D. M., Aghamohammadzadeh, S., Rooij, L., Allwood, E. G., Winder, S. J. and Ayscough, K. R. (2008). Interactions between the yeast SM22 homologue Scp1 and actin demonstrate the importance of actin bundling in endocytosis. *J. Biol. Chem.* **283**, 15037-15046.

Herskovits, J. S., Burgess, C. C., Obar, R. A. and Vallee, R. B. (1993). Effects of mutant rat dynamin on endocytosis. *J. Cell Biol.* **122**, 565-578.

Hinshaw, J. E. and Schmid, S. L. (1995). Dynamin self-assembles into rings suggesting a mechanism for coated vesicle budding. *Nature* **374**, 190-192.

Hoepfner, D., van den Berg, M., Philippsen, P., Tabak, H. F. and Hettema, E. H. (2001). A role for Vps1p, actin, and the Myo2p motor in peroxisome abundance and inheritance in *Saccharomyces cerevisiae*. *J. Cell Biol.* **155**, 979-990.

Huang, K. M., D'Hondt, K., Riezman, H. and Lemmon, S. K. (1999). Clathrin functions in the absence of heterotetrameric adaptors and AP180-related proteins in yeast. *EMBO J.* **18**, 3897-3908.

Huh, W. K., Falvo, J. V., Gerke, L. C., Carroll, A. S., Howson, R. W., Weissman, J. S. and O'Shea, E. K. (2003). Global analysis of protein localization in budding yeast. *Nature* **425**, 686-691.

Itoh, T., Erdmann, K. S., Roux, A., Habermann, B., Werner, H. and De Camilli, P. (2005). Dynamin and the actin cytoskeleton cooperatively regulate plasma membrane invagination by BAR and F-BAR proteins. *Dev. Cell* **9**, 791-804.

Jonsdottir, G. A. and Li, R. (2004). Dynamics of yeast myosin I: Evidence for a possible role in scission of endocytic vesicles. *Curr. Biol.* **14**, 1604-1609.

Kaiser, C., Michaelis, S. and Mitchell, A. (1994). *Methods in Yeast Genetics: a Laboratory Course Manual.* Cold Spring Harbor, NY: Cold Spring Harbor Laboratory Press.

Kaksonen, M., Sun, Y. and Drubin, D. G. (2003). A pathway for association of receptors, adaptors, and actin during endocytic internalization. *Cell* **115**, 475-487.

Kaksonen, M., Toret, C. P. and Drubin, D. G. (2005). A modular design for the clathrin- and actin-mediated endocytosis machinery. *Cell* **123**, 305-320.

Koenig, J. H. and Ikeda, K. (1989). Disappearance and reformation of synaptic vesicle membrane upon transmitter release observed under reversible blockage of membrane retrieval. *J. Neurosci.* **9**, 3844-3860.

Kruchten, A. E. and McNiven, M. A. (2006). Dynamin as a mover and pincher during cell migration and invasion. *J. Cell Sci.* **119**, 1683-1690.

Kuravi, K., Nagotu, S., Krikken, A. M., Sjollema, K., Deckers, M., Erdmann, R., Veenhuis, M. and van der Klei, I. J. (2006). Dynamin-related proteins Vps1p and Dnm1p control peroxisome abundance in *Saccharomyces cerevisiae*. *J. Cell Sci.* **119**, 3994-4001.

Liu, J., Sun, Y. D., Drubin, D. G. and Oster, G. F. (2009). The mechanochemistry of endocytosis. *PLoS Biol.* **7**, e1000204.

Longtine, M. S., McKenzie, A., Demarini, D. J., Shah, N. G., Wach, A., Brachat, A., Philippsen, P. and Pringle, J. R. (1998). Additional modules for versatile and economical PCR-based gene deletion and modification in *Saccharomyces cerevisiae*. *Yeast* **14**, 953-961.

Maldonado-Baez, L., Dores, M. R., Perkins, E. M., Drivas, T. G., Hicke, L. and Wendland, B. (2008). Interaction between epsin/Yap180 adaptors and the scaffolds Ede1/Pan1 is required for endocytosis. *Mol. Biol. Cell* **19**, 2936-2948.

Marks, B., Stowell, M. H. B., Vallis, Y., Mills, I. G., Gibson, A., Hopkins, C. R. and McMahon, H. T. (2001). GTPase activity of dynamin and resulting conformation change are essential for endocytosis. *Nature* **410**, 231-235.

Merrifield, C. J., Feldman, M. E., Wan, L. and Almers, W. (2002) Imaging actin and dynamin recruitment during invagination of single clathrin-coated pits. *Nat. Cell Biol.* **4**, 691-698.

Morton, W. M., Ayscough, K. R. and McLaughlin, P. J. (2000). Latrunculin alters the actin-monomer subunit interface to prevent polymerization. *Nat. Cell Biol.* **2**, 376-378.

Motley, A. M. and Hettema, E. H. (2007). Yeast peroxisomes multiply by growth and division. *J. Cell Biol.* **178**, 399-410.

Nannapaneni, S., Wang, D., Jain, S., Schroeder, B., Highfill, C., Reustle, L., Pittsley, D., Maysent, A., Moulder, S., McDowell, R. et al. (2010). The yeast dynamin-like protein Vps1:*vps1* mutations perturb the internalization and the motility of endocytic vesicles and endosomes via disorganization of the actin cytoskeleton. *Eur. J. Cell Biol.* **89**, 499-508.

Narayanan, R., Leonard, M., Song, B. D., Schmid, S. L. and Ramaswami, M. (2005). An internal GAP domain negatively regulates presynaptic dynamin in vivo: a two-step model for dynamin function. *J. Cell Biol.* **169**, 117-126.

Nothwehr, S. F., Conibear, E. and Stevens, T. H. (1995). Golgi and vacuolar membrane-proteins reach the vacuole in Vps1 mutant yeast cells via the plasma membrane. *J. Cell Biol.* **129**, 35-46.

Ochoa, G. C., Slepnev, V. I., Neff, L., Ringstad, N., Takei, K., Daniell, L., Kim, W., Cao, H., McNiven, M., Baron, R. et al. (2000). A functional link between dynamin and the actin cytoskeleton at podosomes. *J. Cell Biol.* **150**, 377-389.

Peters, C., Baars, T. L., Buhler, S. and Mayer, A. (2004). Mutual control of membrane fission and fusion proteins. *Cell* **119**, 667-678.

Raymond, C. K., Howald-Stevenson, I., Vater, C. A. and Stevens, T. H. (1992). Morphological classification of the yeast vacuolar protein sorting mutants: evidence for a prevacuolar compartment in class E vps mutants. *Mol. Biol. Cell* **3**, 1389-1402.

Robertson, A. S., Smythe, E. and Ayscough, K. R. (2009). Functions of actin in endocytosis. *Cell. Mol. Life Sci.* **66**, 2049-2065.

Rothlisberger, S., Jourdain, I., Johnson, C., Takegawa, K. and Hyams, J. S. (2009). The dynamin-related protein Vps1 regulates vacuole fission, fusion and tubulation in the fission yeast, *Schizosaccharomyces pombe*. *Fungal Genet. Biol.* **46**, 927-935.

Sever, S., Muhlberg, A. B. and Schmid, S. L. (1999). Impairment of dynamin's GAP domain stimulates receptor-mediated endocytosis. *Nature* **398**, 481-486.

Shin, H. W., Takatsu, H., Mukai, H., Munekata, E., Murakami, K. and Nakayama, K. (1999). Intermolecular and interdomain interactions of a dynamin-related GTP-binding protein, Dnm1p/Vps1p-like protein. *J. Biol. Chem.* **274**, 2780-2785.

Shpetner, H. S. and Vallee, R. B. (1989). Identification of dynamin, a novel mechanochemical enzyme that mediates interactions between microtubules. *Cell* **59**, 421-432.

Song, B. D. and Schmid, S. L. (2003). A molecular motor or a regulator? Dynamin's in a class of its own. *Biochemistry* **42**, 1369-1376.

Song, B. D., Leonard, M. and Schmid, S. L. (2004a). Dynamin GTPase domain mutants that differentially affect GTP binding, GTP hydrolysis, and clathrin-mediated endocytosis. *J. Biol. Chem.* **279**, 40431-40436.

Song, B. D., Yarar, D. and Schmid, S. L. (2004b). An assembly-incompetent mutant establishes a requirement for dynamin self-assembly in clathrin-mediated endocytosis in vivo. *Mol. Biol. Cell* **15**, 2243-2252.

Stamenova, S. D., Dunn, R., Adler, A. S. and Hicke, L. (2004). The Rsp5 ubiquitin ligase binds to and ubiquitinates members of the yeast CIN85-endophilin complex, Sla1-Rvs167. *J. Biol. Chem.* **279**, 16017-16025.

Tong, A. H. Y., Evangelista, M., Parsons, A. B., Xu, H., Bader, G. D., Page, N., Robinson, M., Raghibizadeh, S., Hogue, C. W. V., Bussey, H. et al. (2001). Systematic genetic analysis with ordered arrays of yeast deletion mutants. *Science* **294**, 2364-2368.

Toshima, J. Y., Nakanishi, J.-I., Mizuno, K., Toshima, J. and Drubin, D. G. (2009). Requirements for recruitment of a G protein-coupled receptor to clathrin-coated pits in budding yeast. *Mol. Biol. Cell* **20**, 5039-5050.

Van Der Bliek, A. M. and Meyerowitz, E. M. (1991). Dynamin-like protein encoded by the *Drosophila shibire* gene associated with vesicular traffic. *Nature* **351**, 411-414.

Vater, C. A., Raymond, C. K., Ekena, K., Howaldstevenson, I. and Stevens, T. H. (1992). The Vps1 protein, a homolog of dynamin required for vacuolar protein sorting in *Saccharomyces cerevisiae*, is a gtpase with 2 functionally separable domains. *J. Cell Biol.* **119**, 773-786.

Yamada, H., Padilla-Parra, S., Park, S. J., Itoh, T., Chaineau, M., Monaldi, I., Cremona, O., Benfenati, F., De Camilli, P., Coppey-Moisan, M. et al. (2009). Dynamic interaction of amphiphysin with N-WASP regulates actin assembly. *J. Biol. Chem.* **284**, 34244-34256.

Yoon, Y., Pitts, K. R. and McNiven, M. A. (2001). Mammalian dynamin-like protein DLP1 tubulates membranes. *Mol. Biol. Cell* **12**, 2894-2905.

Yu, X. W. and Cai, M. J. (2004). The yeast dynamin-related GTPase Vps1p functions in the organization of the actin cytoskeleton via interaction with Sla1p. *J. Cell Sci.* **117**, 3839-3853.

Supplementary table 1. Yeast strains used in this study

Strain Number	Genotype	Notes
KAY1450	MATα *pep4::HIS3 prbl-Al.6R HIS3 lys2-208 trpl-Δ101 ura3-52 gal2 can1 Vps1Gly$_6$GFP::KanMx-loxP*	Peters et al, 2004
KAY1470	*MATa his3-Δ200, leu2-3/112, ura3-52, trp1-1* Abp1mRFP::HIS3	This study
KAY870	MATa *his3-Δ200, leu2-3/112, ura3-52 Sla1-mRFP::HIS3*	This study
KAY1492	MAT a/α KAY1450 x KAY1470	This study
KAY1493	MAT a/ α KAY1450 x KAY870	This study
KAY684	MATα *SAC6-RFP::kanMX, his3Δ1, leu2Δ0, lys2Δ0, ura3Δ0*	Huh et al, 2003
KAY1368	KAY684 Δ*vps1::LEU2*	This study
KAY723	MATα *SLA2-GFP::HIS3, his3Δ1, leu2Δ0, met15Δ0, ura3Δ0*	Invitrogen
KAY1459	KAY723 Δ*vps1::LEU2*	This study
KAY1320	MATα *ENT1-GFP::HIS3, his3Δ1, leu2Δ0, met15Δ0, ura3Δ0*	Invitrogen
KAY1460	KAY1320 Δ*vps1::LEU2*	This study
KAY757	MATα *LAS17-GFP::HIS3, his3Δ1, leu2Δ0, met15Δ0, ura3Δ0*	Invitrogen
KAY1370	KAY757 Δ*vps1::LEU2*	This study
KAY726	MATα *Rvs167-GFP::HIS3, his3Δ1, leu2Δ0, met15Δ0, ura3Δ0*	Invitrogen
KAY1337	KAY726 Δ*vps1::LEU2*	This study
BY4741	*MATa his3Δ1, leu2Δ0, met15Δ0, ura3Δ0*	Invitrogen
BY4742	*MATa his3Δ1, leu2Δ0, lys2Δ, ura3Δ0*	Invitrogen
KAY1095	MATα *his3Δ1, leu2Δ0, lys2Δ, ura3Δ0 Δvps1::KanMx*	Invitrogen
KAY1098	BY4742 Δ*rvs167::LEU2*	This study
KAY1100	KAY1095 Δ*rvs167::LEU2*	This study
KAY1096	BY4742 Δ*dnm1::KanMx* Δ*vps1::HIS5*	EH lab
KAY1462	BY4742 + integrated GFP-Snc1-SUC2 URA	This study
KAY1535	*MATa his3-Δ200, leu2-3/112, ura3-52, trp1-1 Rvs167-mRFP*	This study
KAY1536	KAY1450 x KAY1535	

Supplementary Table 2. Plasmids used in this study

Plasmid number	Description	Origin/Reference
pKA474	For LEU marked gene deletion	Drubin (Berkeley)
pKA88	Abp1GFP URA	Doyle & Botstein 1996
pHB4	SUC2 5'UTR-ADHpr-NATR-GFP-SNC1-SUC2 (GSS; ADH promoter)	Burston et al, 2009
pEH318/pKA544	URA, CEN with PGKterm	EH lab
pKA677	pKA544+ *VPS1* (inc 320bp 5')	This study
pKA690	pKA544+ *vps1* F585L	This study
pKA692	pKA544+ *vps1* S43N	This study
pKA693	pKA544+ *vps1* R684A	This study
pKA697	pKA544+ *vps1* G188S	This study
pKA698	pKA544+ *vps1* G315D	This study
pKA699	pKA544+ *vps1* T63A	This study
pKA700	pKA544+ *vps1* T183Q	This study
pKA701	pKA544+ *vps1* I649K	This study
pKA702	pKA544+ *vps1* K653A	This study
pKA703	pKA544+ *vps1* K689A	This study
pKA704	pKA544+ *vps1* T183Q, G315D	This study
pKA707	pKA544+ *vps1* R64C	This study